Microbial Fabric Formation in Spring Mounds ("Microbialites") of Alkaline Salt Lakes in the Badain Jaran Sand Sea, PR China

GERNOT ARP*
Institute and Museum of Geology and Paleontology, University of Göttingen, Goldschmidtstraße 3, D-37077 Göttingen, Germany

JÜRGEN HOFMANN
Institute of Geography, Free University of Berlin, Grunewaldstraße 35, D-12165 Berlin, Germany

JOACHIM REITNER
Institute and Museum of Geology and Paleontology, University of Göttingen, Goldschmidtstraße 3, D-37077 Göttingen, Germany

PALAIOS, 1998, V. 13, p. 581–592

The large sandy desert of Badain Jaran Shamo, Inner Mongolia, has several salt lakes located among megadunes with crests as high as 400 m. Most of the lakes are hypo- to hypersaline and alkaline, with pH values between 8.5 and 10. Because of their reef-like aragonitic pinnacles rising from the lake floor, Lake Nuoertu and Lake Huhejaran have been investigated in detail. The porous limestones of the tufa pinnacles ("spring mounds") result from a hydrochemically forced, exopolymer-mediated calcification of cyanobacteria-dominated microbial mats at sublacustrine springs. The development of their enigmatic fabrics is documented for the first time. Sickle-cell-like and bubble-shaped fabrics reflect successive mineralization during degradation, shrinkage of the organic mucus, and gas formation by bacteria. Fossil analogues are known from the Pleistocene and Miocene (Ries-crater lake), but older non-marine, Phanerozoic examples are expected. To the extent that these textures are associated exclusively with alkaline environments, they can be used to test the hypothesis of an alkaline ocean early in Earth history.

INTRODUCTION

Spring mounds are reef-like carbonate build-ups that are linked to groundwater seeps, springs, or vents. This contribution focuses on non-marine, sublacustrine spring mounds. Analogues, known as "tufa pinnacles," are recognized from a number of Pleistocene to Recent alkaline salt lakes (Russel, 1889; Scholl, 1960; Scholl and Taft, 1964; Warren, 1982; Dean and Fouch, 1983; Gasse and Fontes, 1989; Kempe et al., 1991; Council and Bennett, 1993; Benson, 1994). Active pinnacles grow in a highly supersaturated mixing zone of HCO_3^-/CO_3^{2-}-rich lake water and groundwater supplying divalent cations. Owing to the intensive development of microbial mats, which are involved in carbonate precipitation and fabric formation, the resulting carbonate rocks are now generally called "microbialites," or "stromatolites" if laminated fabrics occur.

Supersaturation with respect to calcium carbonate of the macroenvironment is generally a prerequisite for the formation of tufa, as it is for all non-enzymatically precipitated carbonates. Abiotic parameters of carbonate equilibrium, such as physicochemical CO_2 degassing by water agitation and elevated temperature (for fluvial tufa), and mixing of lake and spring water (for tufa pinnacles), are commonly regarded as controlling factors, that, in principle can sufficiently explain tufa formation. Microbial processes promoting $CaCO_3$ supersaturation are autotrophic CO_2-fixation, ammonification, sulfate reduction (Krumbein, 1979) and methanotrophy (Ritger et al., 1987). Only photosynthetic CO_2 removal has been considered in tufa systems. However, $\delta\,^{13}C$ values indicate that tufa carbonate is linked to photosynthesis only to a minor extent (Usdowski et al., 1979; Pentecost and Spiro, 1990).

Because all substrate-water interfaces in nature are colonized by various micro-organisms, and precipitation of $CaCO_3$ does not start before reaching moderate to high supersaturation, one may consider the biological and biochemical properties of these biofilms as crucial factors. Reduced diffusion within the microbially secreted extracellular polymeric substances (EPS) permits the establishment of microenvironments. Apart from the biotic influence on the carbonate equilibrium in micro-niches, biochemical properties of the EPS are expected to influence precipitation significantly in biofilms and microbial mats. This should also be applicable in tufa systems. However, few investigations (Emeis et al., 1987) have taken into account the effect of polysaccharides and amino acids on Ca^{2+} accumulation, $CaCO_3$ nucleation, crystal growth, and fabric formation in tufa carbonates.

The objective of this paper is to demonstrate the crucial influence of extracellular polymeric substances, and their microbial decay, on fabric formation within the hydrochemically driven depositional system of spring-mounds. Further, the potential significance of these characteristic spring-mound carbonates for the reconstruction of the ancient ocean chemistry is discussed.

* Author to whom correspondence should be addressed

0883-1351/98/0013-0581/$3.00

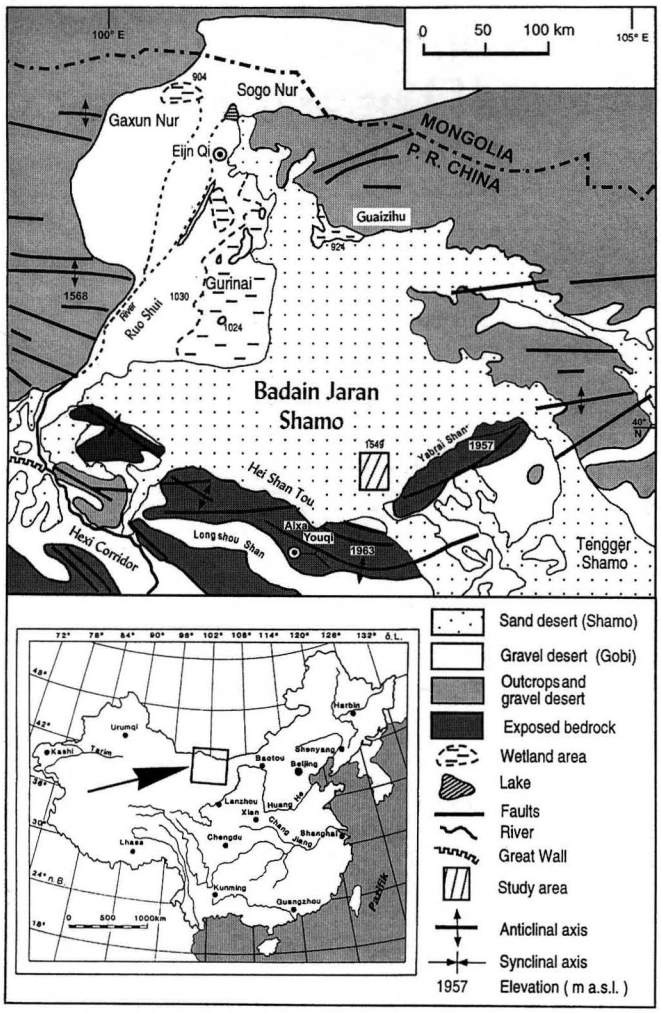

FIGURE 1—Location of the study area in the Badain Jaran Shamo (Inner Mongolia Aut. Reg., PR China).

ENVIRONMENTAL SETTING

During a Chinese-German expedition to the Badain Jaran Desert in 1995 one of us (J.H.) discovered previously unknown, active spring mounds in interdune salt lakes (Hofmann, 1996). The setting is devoid of artificial influence and, hence, provides the rare opportunity to study undisturbed, actively growing spring mounds. Except for Lake Van and Mono Lake pinnacles, which clearly result from present-day carbonate precipitation, most spring mounds are fossil or subfossil structures (e.g., Walker Lake, Pyramid Lake, Winnemucca Lake, Lake Lahontan, Searles Lake. Scholl, 1960; Benson, 1994)

With an area of approximately 44,000 square kilometers, the Badain Jaran Desert (39°20′N to 41°30′N; 100°E to 103°E) is the third largest desert of China. It is situated on the northwestern part of the Alashan plateau (Fig. 1) at elevations between 1000 and 1500 m above sea level. The area is characterized by an extreme continental desert climate with cold winters (Table 1). In contrast to other deserts of Central Asia, more than 50% of the area is covered by megadunes that average 200–300 m in height and occasionally rise above 400 m (Fig. 2). They show a clear orientation along an axis stretching SW-NE, roughly at right angles to the prevailing WNW wind direction. Although the megadunes are sparsely vegetated, they appear to be stable. The interdunal areas in the SE part of the desert are filled with salt plains, wetlands, and more than 100 perennial lakes of different sizes and salinities. There are neither rivers discharging into the lakes nor outlets draining them. Inflow is assumed to be due exclusively to lateral and sublacustrine groundwater movement.

TABLE 1—Climatic data of the study area, Badain Jaran Desert

Annual rainfall	113 mm (SE)–38 min (NW)
Annual potential evaporation	3790 min (W)–2500 mm (E)
Mean annual air temperature	+8.8°C
Lowest monthly mean temperature	−9.9°C (January)
Highest monthly mean temperature	+25.3°C (July)
Winter minimum temperatures	−30.0°C

The distribution of the lakes shows a chessboard-like pattern in the east and a more linear pattern in the west (Zheng et al., 1993). These patterns and the displacement of Cretaceous sedimentary strata at the outcrop of Yikelierbao (39°42′N/102°18′E) in the vicinity of the lakes are evidence of young tectonic events along a fault running NE to SW.

Lakes Nuoertu and Huhejaran, which are two of the largest in the Badain Jaran Desert, were extensively studied in 1995. Both are hypersaline lakes and exhibit pinnacle-shaped spring mounds forming islands or reef-like structures below the lake surface (Fig. 3). In addition, fossil remnants indicating former lake-level highstands were recognized up to 15 m above the present lake level at Lake Nuoertu. For a general overview on Chinese salt lakes, the reader is referred toWilliams (1991) and references therein.

MATERIAL AND METHODS

Water samples for chemical analysis of spring water and lake brines were collected during September and October 1995 in 250 ml and 125 ml polyethylene bottles that had been repeatedly rinsed with distilled water. Electrical

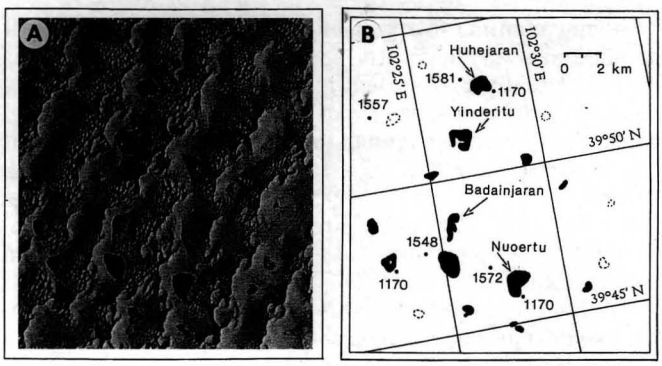

FIGURE 2—LANDSAT-image (A) and sketchmap (B) of the study area showing the investigated lakes Nuoertu and Huhejaran situated between megadunes.

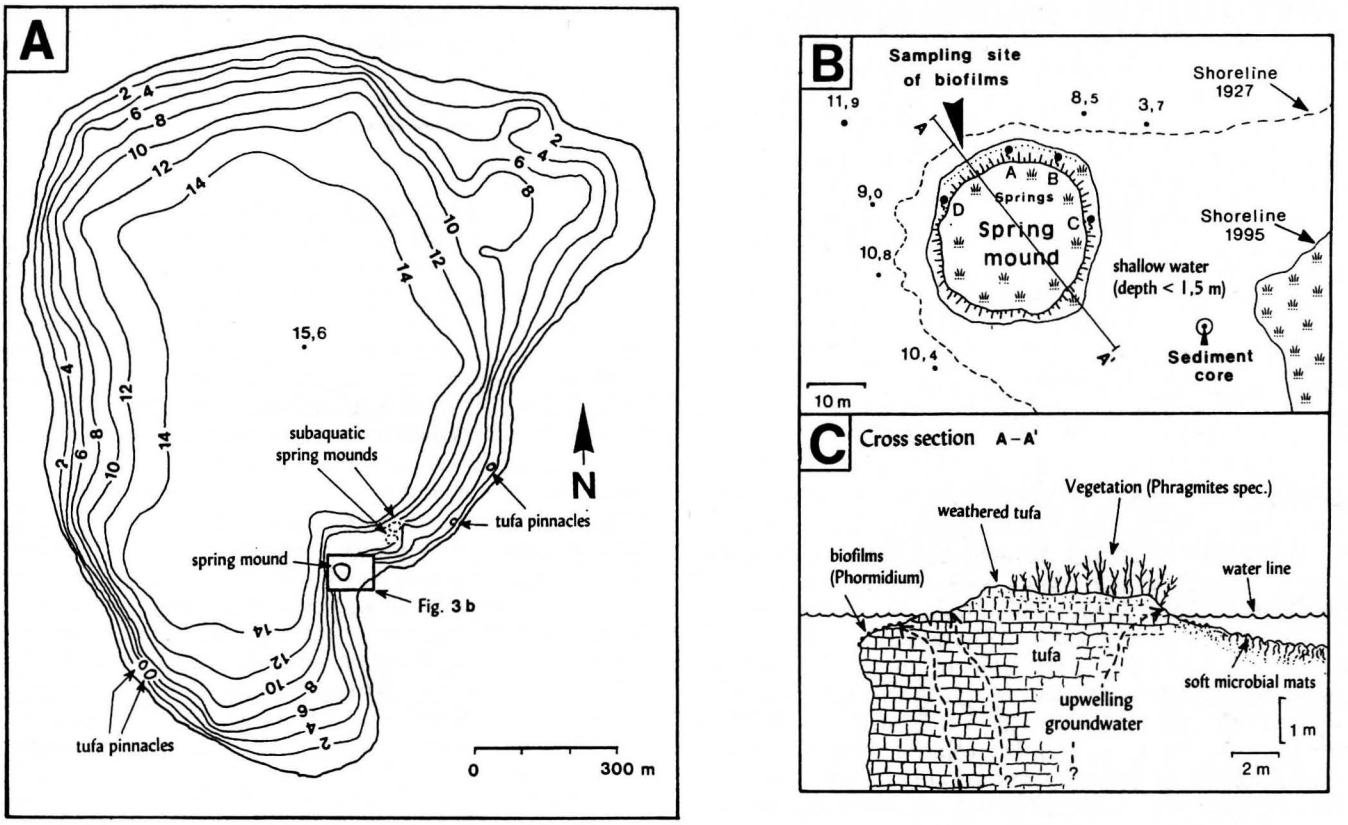

FIGURE 3—Location of sampling site at Lake Nuoertu. (A) Bathymetric map with the location of spring mounds ("tufa pinnacles"). (B) Detailed map of the sampling site and (C) schematic cross section of the Mound. Note that an earthquake in 1927 caused flooding of this shoreline section.

conductivity (EC), pH, temperature, and oxygen concentration were measured in the field using an LF 95 temperature compensating conductivity meter, an Oxi 96 oximeter with salinity correction, and a pH 90 temperature compensating pH meter (WTW Co.). Nitrate, nitrite, and ammonium were analyzed in the field with a portable photometer (model LASA 2-plus, Dr. Lange Co.). All other chemical analyses were carried out in the laboratory of the Institut für Wasser-, Boden- und Lufthygiene (Umweltbundesamt, Berlin) on unfiltered samples. One subsample of each sample was treated with $HgCl_2$ to avoid biochemical alteration processes that might influence unstable parameters (e.g., nitrate) during transport to the laboratory. The major cations and anions were analyzed using an ICP-OES (FISONS Inc.) and ion chromatograph (DIONEX D 12). Water samples of lake brines had to be diluted to 1:10,000 with distilled water because of the high salt content. The carbonate anions HCO_3^- and CO_3^{2-} were determined by titration with HCl and NaOH to obtain the acid and base exchange capacity (Hütter, 1992). The total dissolved solids (TDS) were determined by evaporating to dryness at a specific temperature (105°C).

Samples of microbialites and adherent biofilms were fixed by a mixture consisting of 37% formol, 95% ethanol, and filtrated lake water (1:2:2). Owing to the natural carbonate buffer of the lake water, an additional buffering was not necessary. Subsamples were stained in bulk with toluidin blue O, basic fuchsin, or the fluorochromes calcein, tetracyclin-HCl, or acridine orange in the laboratory to obtain sufficient contrast. After dehydration in graded alcohol series (38–50–70–85–95–100%), the samples were embedded in LR-White resin. Thin sections were cut with a Leica hardpart microtome. After mounting on glass slides, the sections were cut down to 5–10 μm thickness and covered.

The investigation and photographic documentation were carried out using a Zeiss Axiolab microscope with phase contrast and epifluorescence equipment. Nine sections of 2 samples from Lake Huhejaran, 47 sections of 7 spring-mound samples of Lake Nuoertu, and 47 sections of 8 core samples from Lake Nuoertu were examined. The semiquantitative mineralogical composition of 3 samples was determined by X-ray diffractometry.

WATER CHEMISTRY OF LAKE NUOERTU AND HUHEJARAN

The concentration of total dissolved solids for the lake brines is 97.8 g/l for Lake Nuoertu and 107.1 g/l for Lake Huhejaran (Table 2). By contrast, the water of spring mounds in and around the lakes shows very low concentrations of TDS in the range of 0.5 g/l. According to the classification system of Hammer (1983), both lakes are hypersaline, while the springs belong to a freshwater regime. The physicochemical data (Table 3) show a very high alkalinity of 624.5 meq/l (Lake Nuoertu) to 824.9 meq/l (Lake Huhejaran), and high pH values between 8.1 and 10 for both spring and lake water. Dissolved oxygen concen-

TABLE 2—Physicochemical data of spring and lake water of Lake Nuoertu (October 6th, 1995). For localities of spring A–D see Fig. 3B.

	Lake brine lake water	Springwater (spring mound)			
		spring A	spring B	spring C	spring D
Temp. [°C]	17.8	17.1	16.8	17.2	16.5
TDS [g/l]	97.8	0.45	0.43	0.39	0.44
Conductivity [mS/cm]	90.3	0.62	0.59	0.53	0.59
pH	10.0	8.9	8.9	8.8	8.8
O_2 [mg/l]	4.8	5.8	4.4	6.1	
O_2 [%]	73	69	58	73	0.255
discharge [l/s]		0.1	0.15	0.5	0.1

trations range from 4.8 mg/l for lake water to 6.1 mg/l for spring water. The total discharge rates of the examined spring-mounds are not known, but isolated discharge rates between 0.1 and 0.5 l/s were measured at different outflows at the spring mound of Lake Nuoertu (Table 3).

The chemical composition of hypersaline lake brines is dominated by sodium and chloride. In general, the ionic dominance is Na^+ (92 meq%) > K^+ (7 meq%) > Mg^{2+} (1 meq%) : Cl^- (48 meq%) > CO_3^{2-} (33 meq%) > SO_4^{2-} (14 meq%) > HCO_3^- (5 meq%). The relative proportions of the major solutes do not vary remarkably between lakes, although there is a slight difference with regard to the total dissolved solids and alkalinity. High CO_3^{2-} and HCO_3^- concentrations are coupled with very low amounts of K^+, Mg^{2+}, and Ca^{2+}. According to the nomenclature of Eugster and Hardie (1978), the brines of both lakes belong to the Na-Cl-CO_3-(SO_4) type. The anion dominance shows notable quantities of chloride and carbonate. Despite their ionic homogeneity, the Mg/Ca mole ratios are different in the two lakes, with values of 20.8 (Nuoertu) and 2.6 (Huhejaran). The high HCO_3/Ca+Mg mole ratios are similar in both lakes. In addition to the major ions, a number of minor ions have been found. In both lakes, dissolved boron (150–300 mg/l), which is normally present as a trace element only, is a significant component. Significant vertical differences in major ion composition are apparently absent in both lakes, although meromictic lakes (e.g., Lake Yinderitu, see Fig. 2) exist in the vicinity.

The major ions in spring and groundwater are also predominantly Na^+ and Cl^-. In contrast to the lake water, Ca^{2+} and Mg^{2+} are more significant, with Mg/Ca mole ratios ≥1. The pattern of ionic dominance in water of spring mounds is Na^+ (66 meq%) > Mg^{2+} (15 meq%) > Ca^{2+} (14 meq%) > K^+ (5 meq%) : Cl^- (36 meq%) > SO_4^{2-} (27 meq%) > HCO_3^- (24 meq%) > NO_3^- (13 meq%). The total hardness of springwaters (calculated as the total amount of Mg^{2+} and Ca^{2+}) is 0.79 mmol/l at Lake Huhejaran and 1.37 mmol/l at Lake Nuoertu. These waters can be termed soft water. The product of CO_3^{2-} + Ca^{2+} in the mixing zone of springwater and lake brine may lead to supersaturation and consequent precipitation of carbonates. The relatively high nitrate content of spring water is remarkable (0.865 mmol/l or 53.6 mg/l NO_3^-). The source of nitrate is unknown. Nitrate contents of groundwater from wells near Lake Nuoertu are already high. Bacterial decomposition processes within the spring mounds may additionally contribute to nitrate values, but there is no evidence to support this. Minor chemical constituents such as phosphorus are also present.

SPRING MOUNDS AND MICROBIAL MATS OF LAKE NUOERTU AND HUHEJARAN

Spring Mounds of Lake Nuoertu: Structure of Biofilms and Fabric Development

Several spring mounds rising from the lake bottom have been observed in the southern part of Lake Nuoertu (Fig. 3). The largest one forms a small island approximately 30

TABLE 3—Chemical composition of lake brines, springs, and groundwater (Lake Nuoertu and Huhejaran).

	Lake brines (mol/l)		Springwater (mmol/l)		Groundwater (mmol/l)
	Nuoertu (n = 4)	Huhejaran (n = 4)	Nuoertu (spring mound n = 2)	Huhejaran (springs near the shore n = 4)	Nuoertu (n = 2)
Density 20°C [g/cm³]	1.075	1.078		0.9978	0.9981
TDS [g/l]	97.8	107.1	0.5	0.4	0.4
Conductivity[mS/cm]	91.2	94.8	0.68	1.99	0.64
pH	10.0	9.9	8.1	8.6	8.1
Na^+	1.495	1.486	3.255	2.593	2.625
K^+	0.112	0.112	0.245	0.115	0.255
Ca^{2+}	0.000295	0.001715	0.705	0.381	0.730
Mg^{2+}	0.00615	0.004483	0.740	0.405	0.790
NH_4^+					0.12
Cl−	0.786	0.786	2.360	1.318	1.875
SO_4^{2-}	0.113	0.111	1.760	0.505	0.690
NO_3^-	0.000365	0.00062	0.865	0.405	0.475
NO_2^-			0.002	0.002	0.002
HCO_3^-	0.1015	0.1161	1.55	1.63	2.410
CO_3^{2-}	0.2614	0.3544			
PO_4^{3-}	0.000006	0.000004	0.003	0.001	0.001
B	0.011976	0.01249	0.0216	0.0311	0.0211

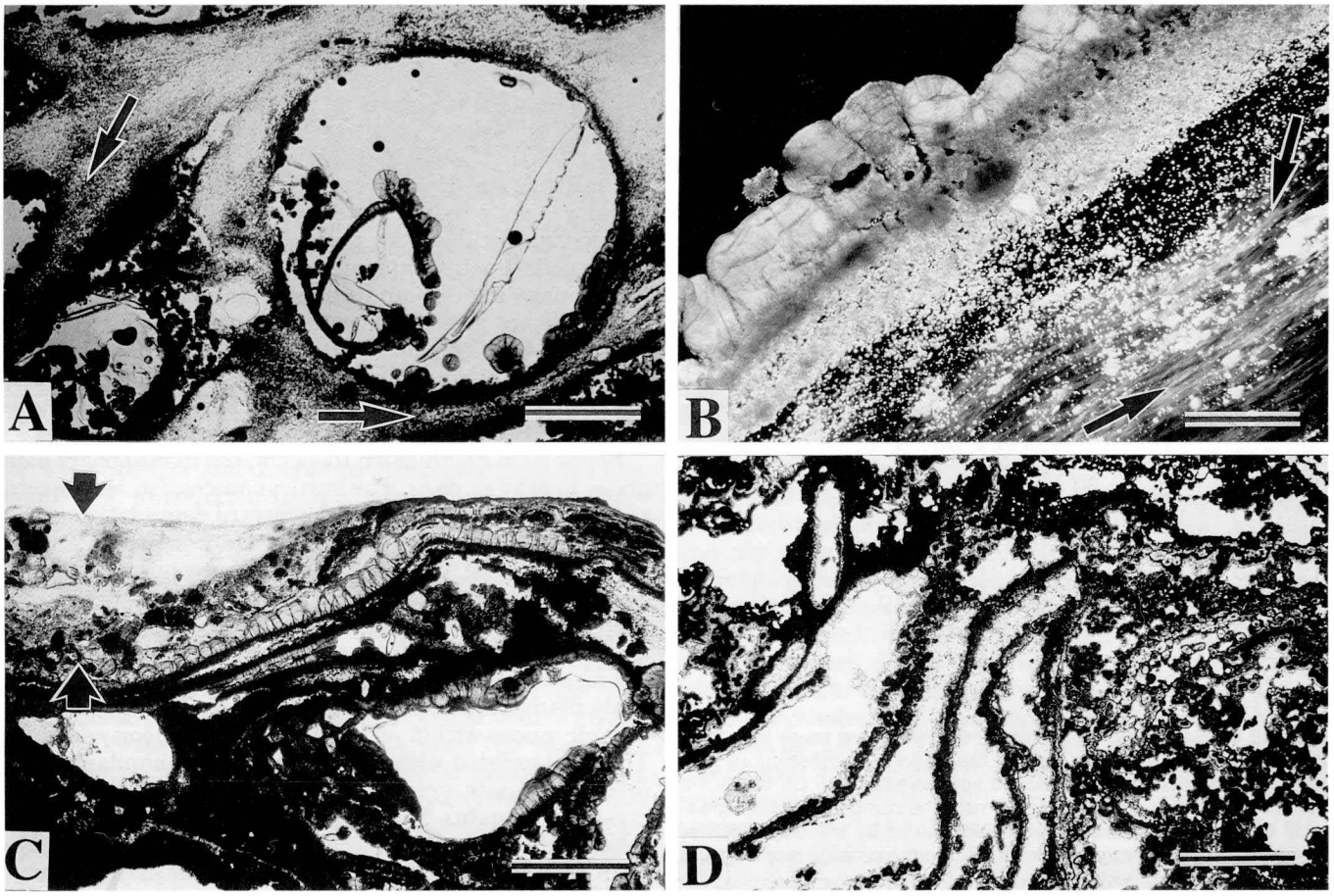

FIGURE 4—Aragonite precipitation and fabric development in spring mound biofilms of Lake Nuoertu. (A) Mucilagenous biofilm of the spring mound surface at the immediate water line, showing initial aragonite precipitates and their spatial concentration (arrows) around shrinkage voids and a gas bubble. Plane light. Scale bar is 1 mm. (B) Formation of microcrystalline laminae at the border of shrinkage voids within the mucilagenous biofilm by spatial concentration and further growth of the initially precipitated aragonite crystals. Note the increased birefringence of successively cleaved polysaccharides in partly dehydrated areas (arrows). Epitaxial "inorganic" precipitation of acicular to botryoidal aragonite is restricted to "mucus-free" surfaces within water-filled voids. Cross polarized light. Scale bar is 250 μm. (C) Complete section of a thin *Phormidium*-biofilm (arrows; stained with acridine orange) on top of spring-mound carbonate at less than 10 cm water depth. Note the highly porous framework composed of irregular stacks of laminae and voids. Plane light. Scale bar is 1 mm. (D) Fossil analogue of the spring-mound carbonates described herein. So-called "sickle-cell-limestones" form meter- to decameter-sized mounds in the Miocene Ries-crater lake, Southern Germany. Plane light. Scale bar is 1 mm.

m in diameter. Active groundwater discharge is evident by a number of freshwater springs at fractures or seeps near the shoreline. Submerged surfaces of this "tufa island" are covered by presently calcifying cyanobacterial biofilms. Tufa samples were taken below water depths of 45 cm, 30 cm, 20 cm, and less than 10 cm to obtain lateral and vertical variations in biofilm structure and fabric of the precipitated carbonate rocks.

Samples from 45-cm water depth show sparsely mineralized biofilms of soft, mucilaginous-fibrous constitution. These are dominated by *Phormidium,* a filamentous cyanobacterium. Small carbonate crystals, 0.25 to 1 μm in size, are distributed in the EPS between cyanobacterial filaments and their sheaths. These small crystals are spindle- and needle-shaped, and are herein called "seed crystals". Detrital particles, such as quartz and feldspar grains, allochthonous carbonate crystals, partly calcified pellets, and arthropod remains, are bound in the biofilm. Early shrinkage of the EPS results in a spatial accumulation of seed crystals to form layers or patches separate from accumulated detrital components.

At 20–30 cm water depth, parts of the biofilm between the living cyanobacterial plexus and the tufa substrate show a high degree of shrinkage and condensation of the EPS with numerous crystal aggregates. The seed crystals tend to be horizontally oriented and dispersed (Fig. 4A, B), but locally clotted or spheroidal aggregates with dark centers also occur. Additionally, lenticular and bubble-shaped voids are developed within the shrinking mucus. The boundaries of the mucus towards the voids are extremely enriched in primary precipitated crystals, that coalesce by further growth to form micritic, irregular laminae (Fig. 4B).

Sections from samples taken below the immediate water line (less than 10 cm water depth) exhibit a similar development 50–350 μm below the living *Phormidium* layer (Fig. 4C). In addition, colonies of *Aphanocapsa* (a coccoid cyanobacterium) are present in the living layer. These

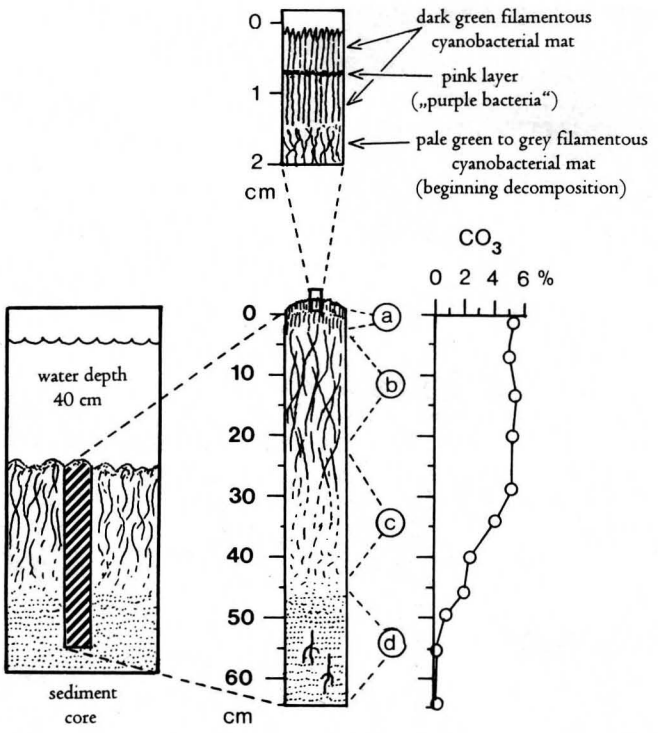

FIGURE 5—Schematic section of the sediment core taken from thick microbial mats of the south bay of Lake Nuoertu. A conspicuous pink layer (purple bacteria) is developed approximately 0.5 cm below the surface of the green cyanobacterial mat. The carbonate content gradually decreases downwards, probably caused by the dissolution of initially precipitated aragonite due to CO_2 production by respiring and possibly fermenting bacteria.

dense colonies of 100–250 μm diameter regularly show a microcrystalline aragonite clot at their centers (Fig. 7D). Pellets and trapped *Artemia* eggs show a micritic impregnation or envelope, respectively. Downwards, the spatial enrichment and growth of primary precipitates leads to solid laminae. Acicular to botryoidal aragonite grows on the laminae in voids and bubbles. The bubbles, which are refilled with water, often show remnants of the collapsed initial microcrystalline wall, followed by acicular veneers (Fig. 4A). As a result, solid micritic laminae with clotted internal fabrics are formed. These laminae are lined by acicular aragonitic cements of open voids. Locally scattered aggregates of bladed, low-Mg calcite are developed as the last phase in the voids. They probably result from freshwater influence (rain water during episodic emersion).

Soft Microbial Mats of the South Bay, Lake Nuoertu: Degradation, Carbonate Precipitation, and Dissolution

Intensively developed, dm-thick microbial sediments have been discovered in the shallow southern bay of Lake Nuoertu. The growth of the microbial mats and sediment accumulation started in 1927, when an earthquake caused a downward movement and flooding of this lake shore section. At 40-cm water depth, a sediment core of 65 cm total length was recovered (Fig. 5).

The uppermost 2 cm of the thick mats are dark-green and consist of a vertically structured, filamentous layer of the cyanobacterium *Phormidium*. *Oscillatoria* is regularly present but of minor abundance. By contrast, coccoid cyanobacteria of the *Aphanocapsa*-group are abundant. Approximately 0.5 cm below its top, a striking pink-colored, 1–2-mm-thick layer has developed. This layer contains large (2 × 5 μm), rod-shaped cells, which are probably purple bacteria. An unequivocal confirmation by the fixed material was not possible. Heterotrophic bacteria (rods, cocci, filaments, spirillae) are present in varying abundance. The mucilagenous-filamentous mat contains detrital particles, including silt- and sand-sized (50–330 μm) quartz and feldspar grains, allochthonous micrite aggregates, and dark calcified pellets (50–80 μm). Carbonate crystals (0.5–4.0 μm) of autochthonous origin are disseminated in the mucus. Their shape is irregular. Patchy crystal aggregates of 100–300 μm size can be observed sporadically.

Below 2 cm depth down to 44 cm, the mat appears pale green to gray in color. The vertical succession of this core section shows a progressive downward degradation of the filamentous cyanobacterial edifice. Only empty sheaths of *Phormidium* are present. Scattered living filaments of *Oscillatoria* are restricted to the uppermost 15 cm of this section. Heterotrophic bacteria (cocci, rods, and occasional filaments and spirillae) occur in abundance. Locally, direct colonization of empty sheaths can be observed. The previously filamentous mat is successively transformed into an organic mucus within which structures are poorly defined. This is associated with the appearance of abundant 0.5 to 5 μm aragonite crystals (irregular to subangular) and crystal aggregates. Microcrystalline aggregates with dark centers are concentrated locally, but they never coalesce to form a friable framework as observed in spring-mound biofilms. Shrinkage processes in the degrading organic mucus lead to a concentration of detrital particles (quartz, feldspar, pellets) and aragonite crystals in some layers. Aragonite crystals generally get smaller downwards. The irregular shape of some aragonite crystals may point to carbonate dissolution.

The deepest core samples (between 44 and 61 cm) probably include shoreline sediments prior to the flooding in 1927. They consist of the decomposed remains of vascular plants. Bacteria (cocci, filaments) are only sporadically visible. The sample contains very little carbonate. Patchy microcrystalline aragonite remnants attached to some detrital quartz grains suggest a redissolution of carbonate. Pellets are numerous, soft, and consist of decomposed plant fibers and small quartz grains.

In summary, the decomposition of cyanobacteria and mucilaginous substances is associated with the formation of small aragonite crystals, but precipitation remains in its initial stage. This might be a consequence of insufficient Ca^{2+}-supply (because no direct groundwater input exists) and possibly intense production of CO_2 by bacterial processes. Deepest sediment samples appear to show evidence for carbonate dissolution.

Spring Mounds of Lake Huhejaran: Composition of Biofilms and Fabric of the Precipitated Carbonates

The general situation of the investigated spring mound in Lake Huhejaran is similar to that of Lake Nuoertu, although the lake water has a slightly higher carbonate alkalinity. This pinnacle rises 10 m from the lake bottom to

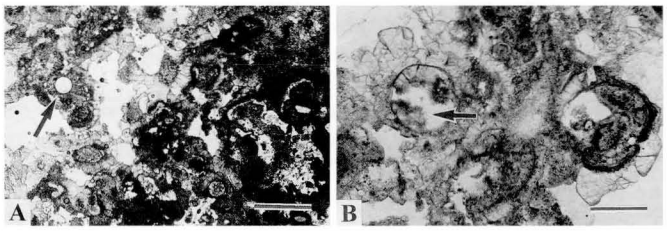

FIGURE 6—Fabric of spring-mound carbonates in Lake Huhejaran. (A) Microcrystalline clots of the primary framework are veneered by "inorganically" precipitated acicular aragonite and patchy low-Mg calcite. Plane light. Scale bar is bar is 1 mm. (B) Arthropod eggs enclosed within microcrystalline to acicular aragonite. Note "inorganically" precipitated, acicular aragonite (arrow) on mucus-free surfaces within the eggs. Subaerial exposure leads to the formation of low-Mg calcite (upper left hand side). Plane light. Scale bar is 250 μm.

the water surface and discharges fresh groundwater. The samples were collected from a mound part, that shows only patchy biofilm development.

As in Lake Nuoertu, cyanobacteria of the genus *Phormidium* are dominant in a biofilm, accompanied by scattered *Oscillatoria* filaments. Colonies of the coccoid cyanobacterium *Aphanocapsa* are restricted to small voids of the microbialite top, associated with microcolonies of heterotrophic bacteria.

Carbonate precipitation is presently restricted to an epitaxial growth of acicular aragonite upon the solid substrate (microbialite). This microbialite is composed of an irregular framework of dark gray cryptocrystalline to microsparitic clots (Fig. 6A, B) with enclosed arthropod eggs and integument fragments, ostracod valves, and quartz and feldspar grains. Elongated voids originate from insect larvae. Brownish spots between the microcrystalline aragonite consist of Fe-hydroxide and organic residues, probably as a result of bacterially-mediated redox reactions at the boundary of anoxic microzones. This fragile, clotted framework is strengthened by microcrystalline to acicular or botryoidal aragonite seams. These delicate aragonite needles are devoid of bacterial colonies, dissolution features, and fractures, indicating that they are presently growing. Only patches show a recrystallization from botryoidal aragonite to a fan-like arrangement of bladed calcite. EPS-mediated calcification has not been observed in our samples because these biofilms are poorly developed. Other spots nearby presumably show calcifying biofilms similar to samples from Lake Nuouertu.

Composition of Microbial Mats

The biofilms and microbial mats of the spring mounds and lake shore are essentially built by filamentous, non-heterocystous cyanobacteria (Fig. 7). The cyanobacterial species within lakes Nuoertu and Huhejaran do not differ significantly. Cyanobacteria are the main primary producers in both lakes. Diatoms are abundant only locally. Most microbial mats in marine and non-marine environments are built by non-heterocystous cyanobacteria (Stal et al., 1994), but the complete lack of heterocystous genera might be linked directly to the high NO_3^--content of spring and lake waters (64.0 and 22.5 mg/l NO_3^-, respectively). A microbiological investigation and identification of non-phototrophic bacteria has not been carried out. Eucaryotic micro-organisms (diatoms, green algae, protozoans) and metazoans were documented only by conventional light microscopy. On the basis of morphological features, five types of cyanobacteria and one other phototrophic bacterium can be distinguished in the fixed material.

A *Phormidum* species (*Phormidium* sp.1), of limited diagnostic characteristics, is the primary producer of spring-mound biofilms and soft microbial mats (Fig. 7A). The trichomes are 0.75 μm in diameter and composed of elongated barrel-shaped cells 3–6 μm long. Occasionally, trichomes have cells up to 8 μm in length, prior to an intercalary cell division. Cell boundaries are slightly constricted. Small inclusions in the cells have been revealed by light microscopy. Each trichome has a very thin sheath.

A second *Phormidium* species (*Phormidium* sp.2) is also present, but is far less common. This form is distinguished from the previous one by its larger trichome diameter of

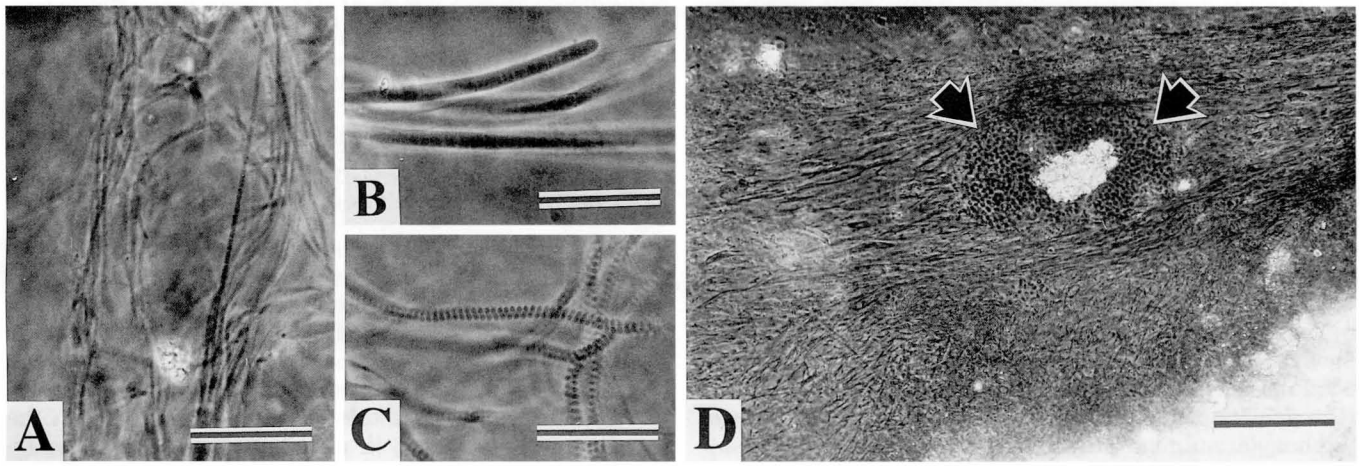

FIGURE 7—Photomicrographs of cyanobacteria from the spring mound biofilms. Phase constrast. Note that no heterocystous genera are present. (A) Small *Phormidium* species essentially form the filamentous plexus of the biofilm. Scale bar is 25 μm. (B) Filaments of "*Oscillatoria*" sp. occur regularily in *Phormidium* mats and biofilms. (C) *Spirulina* cf. *labyrinthiformis* is only occasionally present within the biofilms. Scale bar is 25 μm. (D) 100 μm large colony of *Aphanocapsa* cf. *salina* within the *Phormidium*-dominated biofilm. The center of the colony exhibits newly formed aragonite precipitates. Scale bar is 125 μm.

1.25 to 1.5 μm. The barrel-shaped cells are 2–4 μm long and either unconstricted or only slightly constricted at their cross walls. Cell divisions are intercalary. The sheath is very thin.

Larger trichomes, with a diameter of 3 μm, are tentatively placed in the genus "*Oscillatoria*" (*O.* cf. *tambi*, Fig. 7B). Their cells are 2–2.5 μm long and short barrel-shaped. Cross walls are clearly visible but show no constriction. Biconcave cells are developed locally and a fine transverse striation is superposed ("Ringschwielen," cf. Geitler, 1932). New cross walls are inserted from the sides. Terminal cells do not differ from other trichome cells. *Oscillatoria* shows a very thin sheath.

The helix-shaped filaments of *Spirulina* cf. *labyrinthiformis* are of 2.5 μm total diameter (Fig. 7C). The trichomes are only 0.75 μm in diameter. The whorls of the middle trichome section are very regular, do not touch each other, and are separated by a 0.5- to 0.75-μm-thick space. The trichome is less regularly coiled only at the terminus. Cross walls are not visible and a sheath is lacking. *Spirulina* occurs sporadically in spring-mound biofilms as well as in thick, soft microbial mats of the lake shore.

The only coccoid cyanobacterium present is morphologically classified as *Aphanocapsa* cf. *salina* (Fig. 7D). The cells are spherical with a diameter of 1.5 μm. They are slightly ovoid only prior to binary fission. A diffluent sheath is present but hardly visible. The dark green cells occasionally show a small spherical inclusion. *Aphanocapsa* forms coherent, pigmented colonies without a distinct arrangement of cells.

The conspicuous pink-colored layer, approximately 0.5 cm below the mat top in Lake Nuoertu, reflects abundant nonsulfur purple bacteria, possibly a large *Rhodobacter* species. These bacteria occur between empty cyanobacterial sheaths and few living trichomes. A proper identification on fixed material was not possible.

Higher organisms comprise large protozoans (35–50 μm in size) with a thick flagellum and a cilia ring, and a saprophytic species of nematode, which are generally common in salt- and soda-lakes (e.g., Walker Lake, Great Salt Lake).

ARAGONITE PRECIPITATION AND FABRIC FORMATION AT SPRING MOUNDS

Based on our petrographic observations and theoretical considerations, we propose the following general model of carbonate precipitation and fabric formation in spring mounds (Fig. 8).

(1) Formation of seed crystals—Small (0.25 to 0.5 μm) aragonite crystals grow within the EPS of the microbial mats. Their nucleation occurs without any spatial relation to sheaths of living cyanobacteria. Only locally do bacteria or diatoms serve as nucleation sites. Further growth is inhibited at first by the large buffer capacity of the organic mucus, which means that carboxylate- and sulfate-groups adsorb most of the supplied Ca^{2+} until saturation.

(2) Bacterial transformation and shrinkage of the mucus—Partial dehydration of the organic mucus results in shrinkage and the spatial concentration of seed crystals. Shrinkage also leads to formation of lenticular voids. Bubbles result either from O_2-release by cyanobacteria or from CO_2-formation by bacterial processes (respiration and possibly fermentation).

(3) Surpassing of buffer capacity and epitaxial crystal growth—Initial crystals continue to grow when the Ca^{2+} buffer capacity is exceeded. Clotted microcrystalline precipitates fuse to form irregular laminae or a patchy framework, usually 100–500 μm below the living cyanobacterial biofilm.

(4) Formation of acicular cements in voids—Free growth of aragonite needles occurs at the contact of micritic

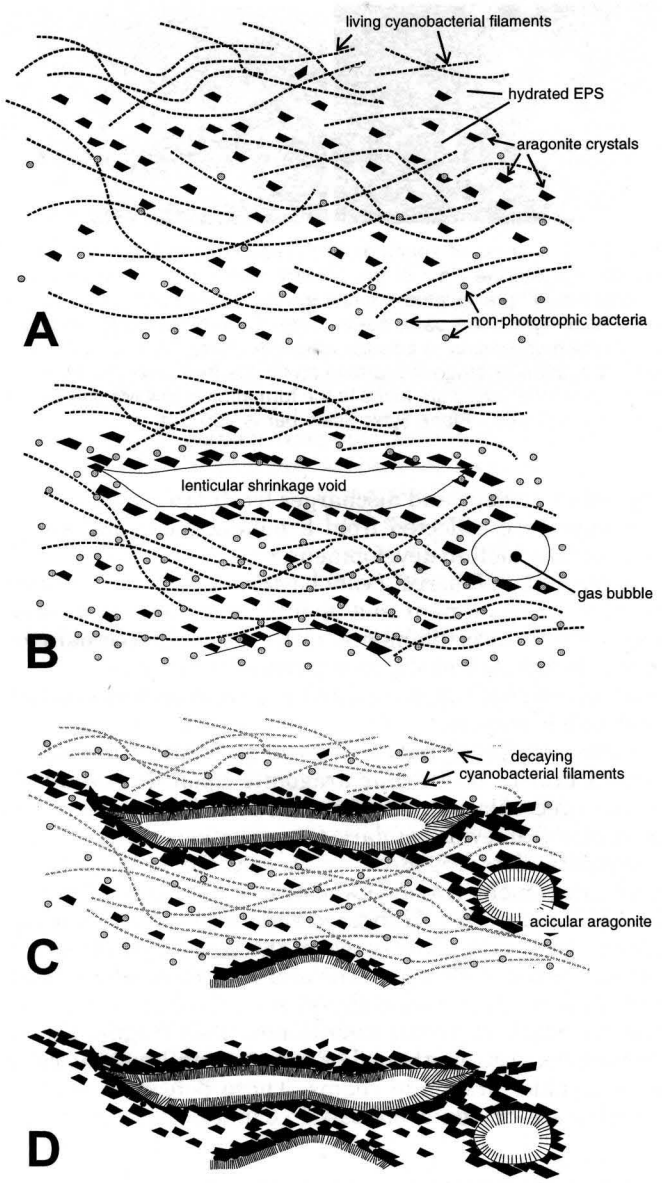

FIGURE 8—Model of aragonite precipitation and fabric formation in mucilaginous biofilms of subaquatic spring mounds in alkaline salt lakes. (A) Cyanobacterial mat with dispersed aragonite seed crystals. (B) Shrinkage of the mucus (EPS), formation of lenticular shrinkage voids and gas bubbles, and growth of aragonite crystals. (C) Decay of cyanobacterial sheath, coalescence of aragonite crystals to cryptocrystalline laminae, and epitaxial growth of acicular aragonite in open voids. (D) Further shrinkage and coalescence to rigid, porous framework.

laminae into open, water-filled voids (lenticular shrinkage voids, bubbles). Consequently, voids are lined by fibrous to botryoidal aragonitic cements.

(5) Subsequent modification—Exposure to meteoric water (heavy rainfall, subaerial exposure) might lead to the formation of bladed, low-Mg-calcite crystals. Also, recrystallization of aragonitic fans to radially arranged, bladed, low-Mg-calcite crystals is considered as an effect of meteoric waters. Dissolution of carbonate associated with the influx of meteoric groundwater is expected in deeper spring-mound parts, but has not been observed in our surface samples. By contrast, precipitation ceases in thick, soft cyanobacterial mats of the lake shore after the initial formation of μm-sized aragonite crystals, because there is no immediate groundwater input.

INORGANIC VERSUS ORGANIC FACTORS CONTROLLING CALCIFICATION

Discussions concerning whether tufa pinnacles are of organic or inorganic origin generally have been fruitless. Considerations should distinguish several aspects of calcium carbonate formation, including the overall physicochemical environment, physico- and biochemical properties of potential nucleation sites, microgradients and physiological activities of micro-organisms, and the growth of crystals and fabric formation.

All spring mounds accrete within a discrete mixing zone of groundwater rich in divalent cations and alkaline lake water. Continuous input of Ca^{2+} ions (34.1 mg/l) into HCO_3^--rich lake water (5524 mg/l) easily exceeds the saturation indices of Ca-carbonate minerals and, consequently, must result in precipitation. This has been well known in principle since the last century (Russel, 1889). Therefore, the general situation is a chemically driven system.

Microbial biofilms/mats consist largely of various polysaccharides (and glycoproteins), which were secreted by micro-organisms to guarantee the attachment and establishment of stable microenvironments (Decho, 1990). Biochemical analyses and histochemical staining procedures demonstrate the acidic nature of the mucus substances, which results from their free carboxylate- and sulfate-groups (Addadi and Weiner, 1989; Reitner, 1993). Both negatively charged groups adsorb divalent cations (e.g., Ca^{2+}) from the liquid phase. As a result, the mucus substances serve as a Ca^{2+} buffer, preventing mineral precipitation at first, an effect that protects micro-organisms and their microenvironments. Nucleation and precipitation does not start until the buffer capacity is surpassed. Retarded nucleation then starts at Ca-ions suitably arranged at the side chains of mucus macromolecules.

Growth of crystals and fabric formation is highly dependent on mucus properties. Dehydration and transformation (enzymatic cleavage, decarboxylation) of components seem to reduce the effectiveness of the buffer in this case and enhance supersaturation, thus promoting crystal growth. Dehydration may result from extracellular enzymatic degradation of long polymers. Highly hydrated, swollen polysaccharide gels are composed of branched or long interwoven molecules, which are more open to contact with water. This is because the exterior of oligo- and polysaccharides are generally very hydrophilic due to their polar OH-groups. In terms of stereochemistry, even a tertiary fold is prevented (Fraústo da Silva and Williams, 1991). These long, hydrated polymer chains are often tightly interwoven to form a complex matrix, which is held intact by ionic interactions (Chanzy and Vuong, 1985). Smaller macromolecules are arranged in shorter elements with far fewer entanglements and interconnections (Chanzy and Vuong, 1985). A great length of macromolecules and the presence of side branches likely reduces the ability of enzymes (e.g., endopolysaccharases) to hydrolyze them (Decho, 1990, p. 123). On the other hand, a high degree of branching enables higher water contents and reduces the possibility of crystallization (Chanzy and Vuong, 1985; Fraústo da Silva and Williams, 1991). Dehydration in deeper parts of biofilms coincides spatially with an increased abundance of heterotrophic bacteria, which probably thrive on these polysaccharides. Their extracellular endo- and exoenzymes are supposed to cleave the long polymers and reduce their branching. Poorly branched polysaccharides are likely to show a more or less increased degree of order and crystallinity. Indeed, dehydration and shrinkage of the mucus proceeds downwards and is occasionally linked with the appearance of a birefringence not seen in fully hydrated areas. These partly dehydrated mucus areas are the loci of initial mineralization. Physicochemical dehydration (T, pH_20) may further support shrinkage, but is only expected during subaerial exposure.

In summary, we propose that endoenzymatic cleavage of highly branched and long polysaccharide molecules leads to H_2O loss and formation of shorter, linear polysaccharide molecules that are more susceptible to regular arrangement and crystallization. Thus, the buffer capacity is further reduced and ion concentrations relative to water content are raised. Finally, at a certain degree of dehydration and supersaturation, the growth of the spatially concentrated primary precipitates proceeds.

Concerning the physiological activity of micro-organisms, a shift in the carbonate equilibrium by photosynthetic CO_2-removal has been shown to be less important in tufa systems (Usdowski et al., 1979), in contrast to massive CO_2-fixation in the whole lake epilimnion (Galat and Jacobsen, 1985) and few published examples of unequivocally photosynthesis-linked cyanobacterial calcification (Thompson and Ferris, 1990; Merz, 1992). Only in the center of dense *Aphanocapsa* colonies did we observe precipitation, which might be linked to their photosynthetic CO_2/HCO_3^--removal (Fig. 7D).

On the contrary, HCO_3^- production by sulfate-reducing bacteria increases alkalinity effectively (Kempe, 1990; Kempe and Kazmierczak, 1990). The investigated biofilms seem to be well oxygenated down to the mineralized surface because living cyanobacteria are distributed throughout. Biofilm EPS has been shown to be highly heterogeneous (Costerton et al., 1995). In general, anaerobic microzones allow the activity of sulfate reduction, methanogenesis, and fermentative reactions. Therefore, we expect fermentation processes (CO_2-formation) and possibly even sulfate-reduction in our mineralizing biofilms. Depending on the concentration of carbonic acid, the pH-buffer system and contaminations, carbonate precipitation should be enhanced by these processes. Organic acids produced by fermentation (acetate, lactate etc.) are not expected to play a significant role with regard to alkalinity and car-

bonate precipitation, because they are immediately used as substrates by heterotrophic bacteria. Thus, they only occur in relatively low concentrations in nature (Lazar et al., 1989).

The fabrics formed at the surface of spring mounds are characterized by laminae and voids, which may result simply from shrinkage and gas bubble formation. Associated spatial enrichment of initial crystals facilitates a coalescence of precipitates to form aggregates or laminae. Gas bubbles are expected only near the air-water interface, because hydrostatic pressure should keep O_2 or CO_2 dissolved at greater depth. Calcified oxygen bubbles of a thermal travertine system have been described by Chafetz et al. (1991). These bubbles form in liquid water. Initial calcium carbonate precipitation (aragonite) could be caused by CO_2-removal from the ambient water into the CO_2-poor oxygen bubble. The initial bubble skin is composed of planar stellate aragonite crystals (followed by aragonite hemispheres and rhombohedral calcite), but no such structures have been found in our sections. CO_2-bubbles, which are veneered and preserved by carbonate, are known from extremely CO_2-rich springs (e.g., Soda Springs/Idaho, personal observations). Trapping in an organic biofilm or mat is prerequisite for their formation. No publications on these CO_2 bubbles within Soda Springs are known to the authors.

The absence of buffering mucus substances upon primary precipitates protruding into voids enables "free" nucleation and growth of "inorganic" crystals (acicular aragonite). Hydrolyzed, "empty" diatoms and green algal cells occasionally are affected in the same way (e.g., Satonda crater lake, observed by G.A.). Internal precipitation precedes external micritic veneering. These rapidly precipitated cements do not allow colonization and biofilm development. In summary, carbonate mineral precipitation in spring-mound biofilms is provided by the adsorption of Ca^{2+}, followed by a retarded nucleation due to its subsequently reduced buffer capacity.

GEOLOGICAL SIGNIFICANCE: SEARCH FOR FOSSIL ANALOGUES

All known spring mounds are restricted to alkaline, more or less saline lakes. Therefore, it is anticipated that detailed analyses of fossil spring-mound carbonates will help to reconstruct the chemistry of ancient lakes. Apart from numerous Quaternary examples, only a few nonthermal spring deposits have been described from the geological record. We assume that this is, at least in part, due to difficulties in their recognition. Highly porous, irregular carbonate frameworks are not easy to describe in a few words, so they usually are classified simply as "tufa." By contrast, Paleozoic travertine deposits of hot springs have been reported from the lower Permian (Karniowice travertine of southern Poland; Szulc and Cwizewicz, 1989) and the upper Devonian/lower Carboniferous (Drummond basin, E-Australia; Walter et al., 1996). A Triassic-Jurassic carbonate hot spring deposit is known from the Hartford Basin of Connecticut ("Coe's quarry"). Mooney et al. (1984) compared the fabrics of these partly hydrothermally altered limestones to "boxwork tufa," a highly porous carbonate rock first described from South Australian coastal salinas (Von der Borch et al., 1977). Redissolution of evaporite crystals (gypsum) caused the open voids between the friable microcrystalline framework in these salinas.

The oldest well-described spring mounds are known from the Miocene crater lake of the Ries impact structure. First considered to be thermal travertine (Gümbel, 1891; Klähn, 1925; Reis, 1926), later as deposits of artesian springs discharging in a hard-water lake (Hollaus, 1969; Bolten, 1977), they are now regarded as build-ups of Ca^{2+}-rich sublacustrine springs into an alkaline lake (Arp, 1995). The observed facies types are essentially identical to those known from active spring mounds (Fig. 4D), although diagenesis has obliterated some of the primary structures.

The proper identification of spring-mound-like carbonate bodies in Precambrian marine sediments might consequently stimulate the discussion on ancient ocean chemistry. Numerous examples of Proterozoic microbialites have been published, mainly well-laminated stromatolitic bioherms (Maslov, 1960; Awramik, 1991, and references therein). None of these seem to be a suitable analogue of our Recent spring mounds; they have large lateral extent and lack spring-related fabrics. Kempe et al. (1991) draw comparisons between tower-shaped spring mounds of Lake Van and Precambrian *Conophyton* stromatolites, based on rough morphological similarities. Although this example is not convincing, irregular Precambrian microbialites have not been considered in the light of the alkaline mound hypothesis. However, if there was an alkaline ocean in early Earth history, it is unlikely that it persisted into Proterozoic times (Grotzinger and Kasting, 1993; Grotzinger, 1994). Late Archean (and early Proterozoic) carbonates (Grotzinger, 1994) might be more promising targets to look for microbialites linked to groundwater input. Given an alkaline Precambrian ocean (Kempe and Degens, 1985), we would expect spring mounds similar to the Recent ones described herein.

CONCLUSIONS

(1) The carbonate spring mounds of Lake Nuoertu and Lake Huhejaran are formed by a physicochemically forced aragonite precipitation at sublacustrine, Ca^{2+}-supplying springs that discharge into an highly alkaline lake water.

(2) Mucus substances of spring-mound biofilms are responsible for the adsorption and spatial fractionation of Ca^{2+}. The alteration of the mucus by the activity of heterotrophic bacteria determines the fabric formation (shrinkage voids and gas bubbles), and the reduction of the Ca^{2+}-buffer capacity. The latter effect finally enables substantial aragonite precipitation.

(3) Calcium carbonate precipitation immediately linked to the physiological activity of cyanobacteria is restricted to the center of dense *Aphanocapsa* colonies.

(4) In well-developed, soft cyanobacterial mats of shallow water areas without immediate groundwater input, the aragonite precipitation ceases after the initial formation of small aragonite crystals. This is due to the large buffering capacity of the mucus, insufficient Ca^{2+}-supply, and possibly CO_2-production by respiring bacteria.

(5) The record of pre-Tertiary spring mounds is sparse, probably owing to a lack of recognition. Their potential

identification in ancient marine settings may stimulate the debate on the development of ocean chemistry during early Earth history.

ACKNOWLEDGMENTS

This publication is contribution No. 6 of the Collaborative Research Center 468 "Wechselwirkungen an geologischen Grenzflächen" at the University of Göttingen (funded by the Deutsche Forschungsgemeinschaft). The expeditionary program was financed by the Deutsche Forschungsgemeinschaft (Ho 1683/1–3) and the Max Planck Association (MPG). Special thanks are due to Prof. Chen Fahu from Lanzhou University and to Prof. Li Baosheng (Guangzhou Normal University) for administrative assistance. Prof. Dr. Jäkel (FU Berlin) is thanked for cartographical support, especially with a large-scale map. We greatly appreciate the hospitality of our Chinese and Mongolian hosts. JR and GA were supported by the DFG projects Re 665–7,12 (Leibnitz Award). We are indebted to Mrs. Annebeck (Berlin) and Mrs. Schmidt (Göttingen) for improving our English. Two anonymous reviewers gave valuable and helpful comments.

REFERENCES

ADDADI, L., and WEINER, S., 1989, Stereochemical and Structural Relations between Macromolecules and Crystalls in Biomineralization: *in* Mann, S., Webb, J., and Williams, R.J.P., eds., Biomineralization: VCH Verlagsgesellschaft, Weinheim, p. 133–156.

ARP, G., 1995, Lacustrine bioherms, spring mounds, and marginal carbonates of the Ries-impact-crater (Miocene, Southern Germany): Facies, v. 33, p. 35–90.

AWRAMIK, S.M., 1991, Archaean and Proterozoic Stromatolites: *in* Riding, R., ed., Calcareous Algae and Stromatolites: Springer-Verlag, Berlin, p. 289–304.

BENSON, L., 1994, Carbonate deposition, Pyramid Lake Subbasin, Nevada: 1. Sequence of formation and elevational distribution of carbonate deposits (Tufas): Palaeogeography, Palaeoclimatology, Palaeoecology, v. 109, p. 55–87.

BOLTEN, R.H., 1977, Die karbonatischen Ablagerungen des obermiozänen Kratersees im Nördlinger Ries: Unpublished PhD Thesis, Ludwig-Maximilians-University, Munich, 228 p.

CHAFETZ, H.S., RUSH, P.F., and UTECH, N.M., 1991, Microenvironmental controls on mineralogy and habit of CaCO3 precipitates: An example from an active travertine system: Sedimentology, v. 38, p.107–126.

CHANZY, H., and VUONG, R., 1985, Ultrastructure and morphology of crystalline polysaccharides: *in* Atkins, E.D.T., ed., Polysaccharides. Topics in Structure and Morphology: VCH Verlagsgesellschaft, Weinheim, p. 41–71.

COSTERTON, J.W., LEWANDOWSKI, Z., CALDWELL, D.E., KORBER, D.R., and LAPPIN-SCOTT, H.M., 1995, Microbial Biofilms: Annual Reviews of Microbiology, v. 49, p. 711–746.

COUNCIL, T.C., and BENNETT, P.C., 1993, Geochemistry of ikaite formation at Mono Lake, California: Implications for the origin of tufa mounds: Geology, v. 21, p. 971–974.

DEAN, W.E., and FOUCH, T.D., 1983, Lacustrine environment: *in* Scholle, P.A., Bebout, D.G., and Moore, H., eds., Carbonate Depositional Environments: American Association of Petroleum Geologists, Memoir No. 33, p. 97–130.

DECHO, A.W., 1990, Microbial exopolymer secretions in ocean environments: Their role(s) in food webs and marine processes: Oceanography and Marine Biology Annual Review, v. 28, p. 73–153.

EMEIS, K.C., RICHNOW, H.H., and KEMPE, S., 1987, Travertine formation in Plitvice National Park, Yugoslavia. Chemical versus biological control: Sedimentology, v. 34, p. 595–609.

EUGSTER, H.P., and HARDIE, L.A., 1978, Saline lakes: *in* Lerman, A., ed., Lakes: Chemistry, Geology, Physics: Springer-Verlag, Berlin, p. 237–293.

FRAÚSTO DA SILVA, J.J.R., and WILLIAMS, R.J.P., 1991, The Biological Chemistry of the Elements. The Inorganic Chemistry of Life: Oxford University Press, Oxford, 561 p.

GALAT, D.L., and JACOBSEN, R.L., 1985, Recurrent aragonite precipitation in saline-alkaline Pyramid Lake, Nevada: Archiv für Hydrobiologie, v. 105, p. 137–159.

GASSE, F., and FONTES, J.C., 1989, Palaeoenvironments and palaeohydrology of a tropical closed lake (Lake Asal, Djibouti) since 10,000 yr B.P.: Palaeogeography, Palaeoclimatology, Palaeoecology, v. 69, p. 67–102.

GEITLER, L., 1932, Cyanophyceae: Rabenhorst's Kryptogamen-Flora von Deutschland, österreich und der Schweiz, v. 14, 2nd ed.: Koeltz Scientific Books (Reprint 1985), Koenigstein, 1196 p.

GROTZINGER, J.P., 1994, Trends in Precambrian carbonate sediments and their implication for understanding evolution: *in* Bengtson, S., ed., Early Life on Earth: Nobel Symposium No. 84, Columbia University Press, New York, p. 245–258.

GROTZINGER, J.P., and KASTING, J.F., 1993, New contraints on Precambrian ocean composition: Journal of Geology, v. 101, p. 235–243.

GÜMBEL, C.W., VON, 1891, Geognostische Beschreibung der Fränkischen Alb (Frankenjura) mit dem anstossenden fränkischen Keupergebiet: Geognostische Beschreibung des Königreichs Bayern. Vierte Abtheilung: Fischer, Kassel, 763 p.

HAMMER, U.T., ed., 1983, Saline lakes: Proceedings of the 2nd International Symposium on athalassic (inland) saline lakes: Developments in Hydrobiology, v. 16, p. 1–264.

HOFMANN, J., 1996, The Lakes in the SE Part of Badain Jaran Shamo, their limnology and geochemistry: Geowissenschaften, v. 14, p. 275–278.

HOLLAUS, E., 1969, Geologische Untersuchungen im Ries. Das Gebiet der Blätter Nördlingen-Ost und Nördlingen-West, mit besonderer Berücksichtigung der Pleistozän-Ablagerungen: Unpublished PhD Thesis, Ludwig-Maximilians University, Munich, 85 p.

HÜTTER, L.A., 1992, Wasser und Wasseruntersuchung: Salle & Sauerländer, Frankfurt am Main, 515 p.

KEMPE, S., 1990, Alkalinity: The link between anaerobic basins and shallow water carbonates?: Naturwissenschaften, v. 77, p. 426–427.

KEMPE, S., and DEGENS, E.T., 1985, An early soda ocean?: Chemical Geology, v. 53, p. 95–108.

KEMPE, S., and KAZMIERCZAK, J., 1990, Chemistry and stromatolites of the sea-linked Satonda Crater Lake, Indonesia: A recent model for the Precambrian sea?: Chemical Geology, v. 81, p. 299–310.

KEMPE, S., KAZMIERCZAK, J., LANDMANN, G., KONUK, T., REIMER, A., and LIPP, A., 1991, Largest known microbialites discovered in Lake Van, Turkey: Nature, v. 349, p. 605–608.

KLÄHN, H., 1925, Paläolimnologische Studien im Ries bei Nördlingen. Vorläufige Mitteilung: Centralblatt für Mineralogie, Geologie und Paläontologie, Abteilung B, v. 1925, p. 320–335.

KRUMBEIN, W.E., 1979, Calcification by bacteria and algae: *in* Trudinger, P.A., and Swaine, D.J., eds., Biogeochemical Cycling of Mineral-Forming Elements: Studies in Environmental Science, v. 3, Elsevier, Amsterdam, p. 47–68.

LAZAR, B., JAVOR, B., and EREZ, J., 1989, Total alkalinity in marine-derived brines and pore waters associated with microbial mats: *in* Cohen, Y., and Rosenberg, E., eds., Microbial Mats. Physiological Ecology of Benthic Microbial Communities: American Society for Microbiology, Washington, D.C., p. 84–93.

MASLOV, V.P., 1960, Stromatoliti: Trudy Instituta Geologiceskich Akademija Nauk, Moskva, v. 41, 188 p.(in Russian).

MERZ, M., 1992, The biology of carbonate precipitation by cyanobacteria: Facies, v. 26, p. 81–102.

MOONEY, J., STEINEN, R., and GRAY, N., 1984, A Mesozoic carbonate hot spring deposit, Coe's Quarry, North Branford, Connecticut: Geological Society of America, Abstracts with Programs, v. 16, p. 52.

PENTECOST, A., and SPIRO, B., 1990, Stable carbon and oxygen isotope composition of calcites associated with modern freshwater cyanobacteria and algae: Geomicrobiology Journal, v. 8, p. 17–26

REIS, O.M., 1926, Zusammenfassung über die im Ries südlich von

Nördlingen auftretenden Süßwasserkalke und ihre Entstehung: Jahresberichte und Mitteilungen des oberrheinischen geologischen Vereins, Neue Folge, v. 14 (1925), p. 176–190.

REITNER, J., 1993, Modern cryptic microbialite/metazoan facies from Lizard Island (Great Barrier Reef, Australia). Formation and concepts: Facies, v. 29, p. 3–40.

RITGER, S., CARSON, B., and SUESS, E., 1987, Methane-derived autigenic carbonates formed by subduction-induced pore-water expulsion along the Oregon/Washington margin: Geological Society of America Bulletin, v. 98, p. 147–156.

RUSSEL, I.C., 1889, Quarternary history of the Mono Valley, California: Eighth Annual Report of the United States Geological Survey (Reprint 1984, Lee Vining), p. 262–394.

SCHOLL, D.W., 1960, Pleistocene algal pinnacles at Searles lake, California: Journal of Sedimentary Petrology, v. 30, p. 414–431.

SCHOLL, D.W., and TAFT, W.H., 1964, Algae, contributors to the formation of calcareous tufa, Mono Lake, California: Journal of Sedimentary Petrology, v. 34, p. 309–319.

STAL, L.J., PAERL, H.W., BEBOUT, B., and VILLBRANT, M., 1994, Heterocystous versus non-heterocystous cyanobacteria in microbial mats: *in* Stal, L.J., and Caumette, P., eds., Microbial Mats. Structure, Development and Environmental Significance: NATO ASI Series, G, v. 35, p. 403–414.

SZULC, J., and CWIZEWICZ, M., 1989, The lower Permian freshwater carbonates of the Slakow Graben, southern Poland: Sedimentary facies context and stable isotope study: Palaeogeography, Palaeoclimatology, Palaeoecology, v. 70, p. 107–120.

THOMPSON, J.B., and FERRIS, F.G., 1990, Cyanobacterial precipitation of gypsum, calcite, and magnesite from natural alkaline lake water: Geology, v. 18, p. 995–998.

USDOWSKI, E., HOEFS, J., and MENSCHEL, G., 1979, Relationship between ^{13}C and ^{18}O fractionation and changes in major element composition in a Recent calcite-depositing spring—A model of chemical variations with inorganic $CaCO_3$ precipitation: Earth and Planetary Science Letters, v. 42, p. 267–276.

VON DER BORCH, C.C., BOLTON, B., and WARREN, J.K., 1977, Environmetal setting and microstructure of subfossil lithified stromatolites associated with evaporites, Marion Lake, South Australia: Sedimentology, v. 24, p. 693–708.

WALTER, M.R., DESMARAIS, D., FARMER, J., and HINMAN, N., 1996, Lithofacies and biofacies of Mid-Paleozoic thermal spring deposits in the Drummond basin, Queensland, Australia: Palaios, v. 11, p. 497–518.

WARREN, J.K., 1982, The hydrological significance of Holocene tepees, stromatolites, and boxwork limestones in coastal salinas in south Australia: Journal of Sedimentary Petrology, v. 52, p. 1171–1201.

WILLIAMS, W.D., 1991, Chinese and Mongolian saline lakes: A limnological overview: Hydrobiologia, v. 210, p. 39–66.

ZHENG, M., TANG, J., LIU, J., and ZHANG, F., 1993, Chinese saline lakes: Hydrobiologia, v. 267, p. 23–36.

ACCEPTED JULY 22, 1998